Universal Bound States with Bose-Fermi Duality in Microwave-Shielded Ultracold Molecules

Tingting Shi,[1,*] Haitian Wang,[1,2,*] and Xiaoling Cui[1,†]
[1]Beijing National Laboratory for Condensed Matter Physics, Institute of Physics, Chinese Academy of Sciences, Beijing 100190, China
[2]School of Physical Sciences, University of Chinese Academy of Sciences, Beijing 100049, China

(Received 13 June 2025; revised 28 September 2025; accepted 9 January 2026; published 26 January 2026)

We report universal bound states of microwave-shielded ultracold molecules that solely depend on the strengths of long-range dipolar interaction and microwave coupling. Under a highly elliptic microwave field, few-molecule scatterings in three dimensions are shown to be governed by effective one-dimensional (1D) models, which well reproduce the tetratomic bound state and the Born-Oppenheimer potential in three-molecule sector. For hexatomic systems comprising three identical molecules, we find a much deeper bound state than the tetratomic one, with binding energy exceeding twice the latter. Strikingly, these bound states display Bose-Fermi duality as facilitated by the effective 1D scattering with a large repulsive core from angular fluctuations. For large molecule ensembles, our results suggest the formation of elongated self-bound droplets with crystalline patterns in both bosonic and fermionic molecules.

DOI: 10.1103/hcwf-tk6c

As an ideal platform for quantum simulation with strong long-range interactions, ultracold polar molecules have recently achieved great developments due to the application of microwave shielding [1–11]. With this technique, intermolecule potential shows, apart from an anisotropic long-range tail, a large repulsive shielding core (spanning hundreds to thousands of Bohr radii) that efficiently suppresses two-body losses. This facilitates the realizations of Fermi degenerate gas of NaK molecules [4] and Bose-Einstein condensation of NaCs [9,10] and NaRb [11] molecules. Further tuning the microwave ellipticity enhances intermolecule attraction, leading to scattering resonance [5] and field-linked tetratomic molecules [6] observed in NaK molecular gas. Theoretically, interesting many-body phases of self-bound bosonic droplets [12–15] and pairing fermion superfluids [16] have been revealed, with the former recently explored in experiments [10,11]. However, in the fundamental few-body level, despite significant progress in two-body (or two-molecule) properties under shielding potentials [16–22], intriguing few-body phenomena beyond two-body ones remain largely unexplored [23,24].

Few-body physics has been extensively studied in ultracold atomic systems with short-range interactions [25–27], where many fascinating cluster bound states were discovered. For instance, Efimov states [28,29], characterized by discrete scaling symmetry and energy sensitivity to short-range parameters, dominate in identical bosons, three distinguishable particles, and highly mass-imbalanced fermion mixtures, often driving atom losses. In contrast, universal bound states, irrelevant to short-range details and stable against inelastic collision, exist in fermion mixtures with intermediate mass imbalance [30–38] and have been shown to induce novel quantum phases with high-order correlations [39–43]. How these distinct bound states behave in long-range interacting polar molecules is an interesting yet challenging problem. Along this direction, previous theories have investigated Efimov physics for three particles interacting with anisotropic long-range and isotropic short-range potentials [44–46]. Such potentials, however, are substantially different from those in microwave-shielded polar molecules. In particular, a large dipole length and a large repulsive shielding core in the latter case may support a new type of universal clusters—a possibility that demands rigorous exploration.

In this Letter, we present the first theoretical investigation of hexatomic (three-molecule) bound state in microwave-shielded 3D polar molecules. To maximize binding strength, we consider the microwave field linearly polarized along y (with elliptic angle $\xi = \pi/4$). Effective one-dimensional (1D) models are established for few-molecule scattering in 3D, with effective potentials containing a long-range $-r^{-3}$ attraction and a r^{-4} repulsive core from angular fluctuations; see illustration in Fig. 1. These models well reproduce tetratomic bound states as well as the Born-Oppenheimer potential in three-molecule sector. Applying to three identical molecules, we find the hexatomic bound state is more favored than the tetratomic state, with binding energy exceeding twice the latter. All these states are universal, in that their properties only depend on physical

*These authors contributed equally to this work.
†Contact author: xlcui@iphy.ac.cn

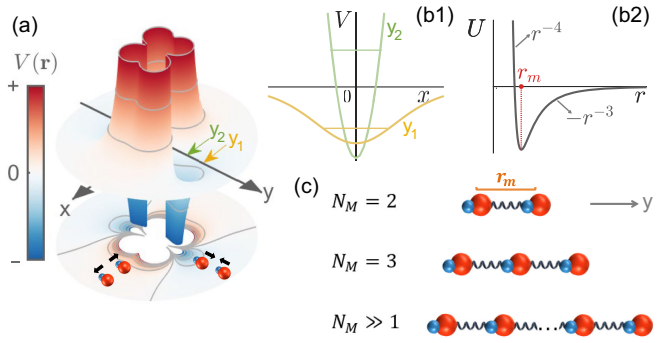

FIG. 1. Schematics of interaction potentials and bound states of polar molecules shielded by a highly elliptic microwave field. (a) Interaction potential $V(\mathbf{r})$ at x-y plane ($z = 0$). (b1) Slices of V at different y [$y_1 > y_2$, as marked by arrows in (a)]. Fluctuations along x ($\sim\delta\phi$) lead to a zero-point energy and effectively upshift the potential to horizontal level. The resulting effective potential $U(r \equiv |y|)$ is plotted in (b2), showing a long-range attraction ($-r^{-3}$) and a repulsive core (r^{-4}) from angular fluctuations. Its minimum is located at r_m. (c) Ground state distribution of bosonic or fermionic molecules with number N_M. They are all bound states aligned along y with typical intermolecule distance r_m.

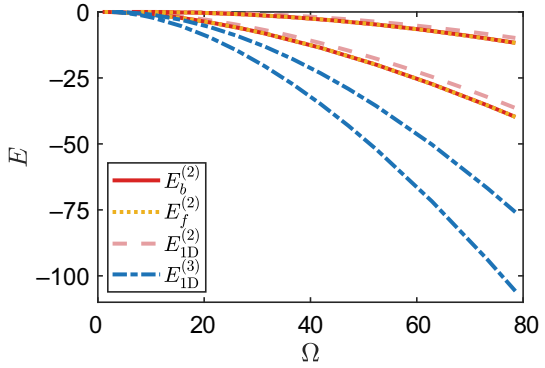

FIG. 2. Binding energies of two and three identical molecules as functions of microwave coupling Ω. Red solid and yellow dotted lines show exact tetratomic energies of bosonic ($E_b^{(2)}$) and fermionic ($E_f^{(2)}$) systems, in comparison to pink dashed lines from the effective 1D model ($E_{1D}^{(2)}$). Blue dash-dotted lines show hexatomic energies from the effective 1D model ($E_{1D}^{(3)}$). For each case, we show the two lowest energy levels. The units of E and Ω are E_u and $E_u/\hbar$.

parameters of long-range dipolar strength and microwave coupling. Importantly, effective 1D scattering with a large repulsive core also facilitates the Bose-Fermi duality of these bound states, i.e., their energies and spatial densities are identical between bosonic and fermionic systems. Extending to large ensembles, our results suggest the formation of elongated self-bound droplets with crystalline pattern in both bosonic and fermionic molecules.

We adopt the interaction potential of microwave-shielded molecules [16] and extrapolate it to elliptic angle $\xi = \pi/4$, where the microwave field $\mathbf{E} = Ee^{i(kz-\omega t)}(\mathbf{e}_+ \cos\xi + \mathbf{e}_- \sin\xi) + \text{c.c.}$ [with $\mathbf{e}_\pm = \mp(\mathbf{e}_x \pm i\mathbf{e}_y)$] is linearly polarized along y and

$$V(\mathbf{r}) = \frac{C_3}{r^3}\left(3\cos^2\theta - 1 + 3\sin^2\theta\cos(2\phi)\right) + \frac{C_6}{r^6}\left(\sin^2\theta\sin^2(2\phi) + \sin^2(2\theta)\sin^4\phi\right). \quad (1)$$

Here $\mathbf{r} = (r, \theta, \phi)$ is the intermolecule distance; $C_3 = [d^2/48\pi\epsilon_0(1+\delta_r^2)]$, $C_6 = [d^4/128\pi^2\epsilon_0^2\Omega(1+\delta_r^2)^{3/2}]$ ($\delta_r = (|\delta|/\Omega)$) with Ω and δ, respectively, denoting the coupling and detuning of the microwave field; d is the dipole moment that defines dipole length $l_d \equiv (m/\hbar^2)[d^2/48\pi\epsilon_0]$. NaK [4–6], NaRb [7], and NaCs [8,9] molecules all have large dipole lengths $l_d/(10^4 a_0) \approx 1.1$, 2.6, 8.3 ($a_0$ is the Bohr radius). In this Letter, we assume a small $\delta_r = 0.2$ and take the length and energy units as $l_u = l_d/20$ and $E_u = (\hbar^2/ml_u^2)$. For NaK, this gives $l_u \approx 550a_0$ and $\hbar\Omega/E_u \approx 52$ at a typical $\Omega = (2\pi)10$ MHz.

As shown in Fig. 1(a), $V(\mathbf{r})$ is extremely anisotropic: it is fully attractive ($= -4C_3/r^3$) along y while fully repulsive ($= 2C_3/r^3$) along x (or z), and the repulsion $\sim C_6/r^6$ takes place in general directions except x, y, z. Among all ξ, the present case ($\xi = \pi/4$) has the most pronounced attraction along y and thus most favors bound state formation, as also inferred from a recent NaK experiment [6].

To begin with, we exactly solve the tetratomic binding energies of bosonic ($E_b^{(2)}$) and fermionic ($E_f^{(2)}$) molecules by diagonalizing their relative Hamiltonian $H^{(2)} = -\hbar^2\nabla_{\mathbf{r}}^2/m + V(\mathbf{r})$ in momentum $\{k\}$ and angular momentum $\{lm\}$ space (see Supplemental Material [47]). Figure 2 shows $E_{b,f}^{(2)}$ for the two lowest bound states, which emerge one by one as increasing Ω. Remarkably, despite distinct $\{klm\}$ compositions in bosonic and fermionic solutions, $E_b^{(2)}$ and $E_f^{(2)}$ are almost identical, with only clear deviations near their emergence [47]. Their typical wave functions $\Psi_{b,f}^{(2)}(\mathbf{r})$ are shown in Figs. 3(a1) and 3(a2): although they have opposite symmetries in two systems, their absolute values are identical—both peak at finite y and vanish at $\mathbf{r} = 0$.

To understand the above phenomena, we study the effective scattering of two molecules along the y direction. Treat any angular deviations from y as small fluctuations,

$$\delta\theta \equiv \theta - \pi/2, \qquad \delta\phi \equiv \phi - \phi_0, \quad (2)$$

with $\phi_0 = \pm\pi/2$, we can expand $V(\mathbf{r})$ up to the lowest fluctuation order $\sim\delta\theta^2, \delta\phi^2$. Together with the kinetic term, $H^{(2)}$ then reduces to two independent harmonic oscillators with respect to $\delta\theta$ and $\delta\phi$ [47]. Further following the adiabatic representation [48–50], we write the tetratomic state as $\Psi^{(2)}(\mathbf{r}) = (1/r)\sum_\nu F_\nu(y)\psi_\nu(y; \delta\theta, \delta\phi)$, with

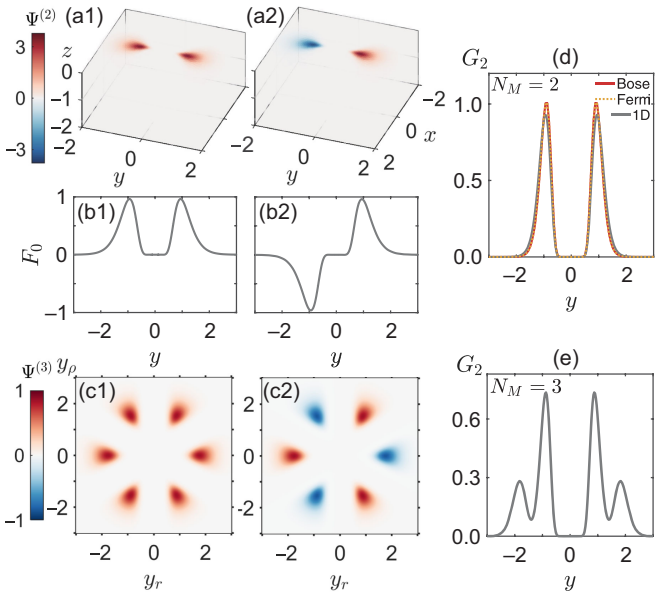

FIG. 3. Bose-Fermi duality of tetratomic and hexatomic bound states at $\hbar\Omega/E_u = 52$. (a1),(a2) and (b1),(b2) show wave functions of the lowest tetratomic states, respectively, from exact solution and effective 1D model. (c1),(c2) Wave functions of the lowest hexatomic states from the effective 1D model. (a1),(b1), (c1) For bosonic molecules and (a2),(b2),(c2) are for fermionic ones. (d),(e) Density correlation functions $G_2(y)$ for tetratomic and hexatomic states. (d) Exact results of bosonic (red solid) and fermionic (yellow dotted) systems are compared with those from the effective 1D model (gray solid). Here the length unit is l_u.

$y = r\sin\phi_0$ the reduced coordinate and ψ_ν the νth eigenstate of harmonic oscillators. Neglecting the off-diagonal couplings between different ν, we obtain the reduced 1D equation for the ground state ($\nu = 0$),

$$\left(-\frac{\hbar^2}{m}\frac{\partial^2}{\partial y^2} + U^{(2)}(|y|)\right)F_0(y) = E_{1D}^{(2)}F_0(y), \tag{3}$$

with ($r \equiv |y|$)

$$U^{(2)}(r) = -\frac{4C_3}{r^3} + \sqrt{\frac{4\hbar^2}{m}\left(\frac{6C_3}{r^5} + \frac{4C_6}{r^8}\right)}. \tag{4}$$

In this way, F_0 and $U^{(2)}$ can be viewed as the reduced wave function and potential in effective 1D. $U^{(2)}$ features a long-range attraction $\sim -r^{-3}$ and a repulsive core $\sim r^{-4}$ that stems from zero-point energy of angular fluctuations [Figs. 1(b1) and 1(b2)]. Physically, such r^{-4} repulsion originates from the interplay of kinetic motion and C_6/r^6 shielding potential, which is very robust and applicable to general ξ. Clearly, this repulsion dominates at small r and effectively forbids two molecules coming close, as evidenced by the vanishing of $F_0(y = 0)$ and $\Psi^{(2)}(\mathbf{r} = 0)$ in Figs. 3(a1)–3(b2), regardless of the statistics of these molecules. Therefore, the bosonic and fermionic systems share identical energies and spatial densities, while the statistics just determine the symmetry of their wave functions. This can be viewed as an extension of Bose-Fermi duality from 1D short-range interacting systems [51,52] to 3D polar molecules with anisotropic long-range interaction. Similar phenomenon has also been indicated for Efimov trimers in dipolar systems [46].

As shown in Fig. 2, $E_{1D}^{(2)}$ produced by Eq. (3) match well with exact $E_{b,f}^{(2)}$ across a wide range of $\hbar\Omega/E_u$. The Bose-Fermi duality can be probed through the density correlation function along y,

$$G_2(y) \equiv \langle n(0)n(y)\rangle, \tag{5}$$

which follows $|F_0(y)|^2$ from the effective 1D model and $\int dxdz|\Psi_{b,f}^{(2)}(\mathbf{r})|^2$ from the exact 3D result. Figure 3(d) shows that these G_2 agree excellently with each other. In fact, the 1D and 3D wave functions match very well over a wide range of Ω, with overlap $> 97\%$ for $\hbar\Omega/E_u > 10$ [47]. These agreements demonstrate the validity of effective 1D treatment in tetratomic problem.

Now we come to hexatomic system of three molecules. A key issue here is to understand the effect of a third molecule, in particular, whether it can bring a scale-invariant $\sim -R^{-2}$ potential as in Efimov physics [25–27]. A physically transparent way to approach it is from the Born-Oppenheimer (BO) limit, by studying the induced heavy-heavy potential by a light object [53]. Importantly, here we can also use BO analysis to benchmark the effective 1D approach to the hexatomic problem.

For a light molecule ($\mathbf{r}$) interacting with two heavy ones ($\pm\mathbf{R}/2$) via microwave-shielded potential, we have exactly diagonalized its Hamiltonian $H_L = -(\hbar^2/2m)\nabla_{\mathbf{r}}^2 + V[\mathbf{r} - (\mathbf{R}/2)] + V[\mathbf{r} + (\mathbf{R}/2)]$ [47] and obtained the eigenenergy $V_{\mathrm{BO}}(\mathbf{R})$, which is exactly the light-induced heavy-heavy potential. In Fig. 4, we plot out V_{BO} for different orientations of $\mathbf{R}$ at a typical Ω, where the effective 1D approach works well to tetratomic problem. We can see $V_{\mathrm{BO}}(\mathbf{R})$ exhibits strong anisotropy inherited from the microwave shielding: it is the lowest for $\mathbf{R}$ along y, while much higher along x or z. Details of $V_{\mathrm{BO}}(\mathbf{R})$ can be found in Supplemental Material [47]. An important message here is that, for all $\mathbf{R}$, we do not observe $-R^{-2}$ behavior in V_{BO}, suggesting the Efimov physics to be greatly suppressed in this case.

The BO potential for $\mathbf{R}$ along y can be well understood from effective 1D theory. Assume small angular fluctuations of $\mathbf{r}$ from y direction, we can expand $H_L(\mathbf{r})$ up to the lowest fluctuation order and extract the zero-point energy. This contributes to a repulsive force in the effective 1D potential [47],

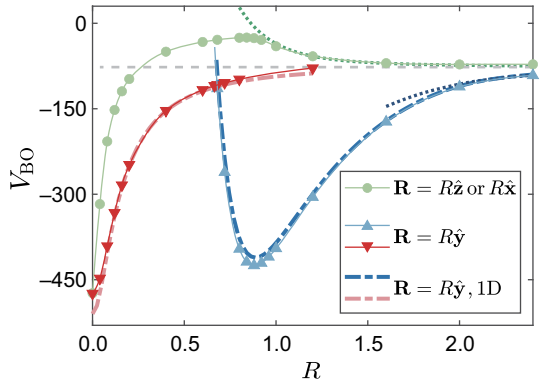

FIG. 4. Light-induced heavy-heavy potential $V_{\rm BO}(R \equiv |\mathbf{R}|)$ in the Born-Oppenheimer limit. Here $\hbar\Omega/E_u = 52$, and the gray horizontal line marks the binding energy of one heavy-light pair. For $\mathbf{R}$ along y, we show two orthogonal levels of $V_{\rm BO}$ (blue and red triangles), while for $\mathbf{R}$ along x or z (equivalent), we show the lowest $V_{\rm BO}$ (green circle). Dashed lines are results from the effective 1D model [Eq. (6)]. Dotted lines at large R show mean-field energies between a heavy-light pair and the rest light molecule [47]. The length and energy units are, respectively, l_u and E_u.

$$U_L(y) = -4C_3\left(\frac{1}{|y_-|^3} + \frac{1}{|y_+|^3}\right) + u_L(y), \tag{6}$$

where $y = r\sin\phi_0$, $y_\pm = y \pm R/2$, and u_L is the induced repulsive force. At $y_\pm \to 0$, $u_L \sim |y_\pm|^{-4}$, signifying a strong repulsion between a heavy-light pair at short distance. This shows the robustness of r^{-4} repulsive core, as established in both two- and three-molecule scattering sectors. As shown in Fig. 4, $V_{\rm BO}$ from effective 1D theory fit exceedingly well with exact results, demonstrating the validity of 1D treatment to hexatomic system.

Finally, we turn to three identical molecules. A similar problem with a shielding potential has been studied in 2D [23]. However, the 3D case is notoriously difficult to solve due to larger Hilbert space and time-consuming computation of long-range coupling strengths. To overcome these difficulties, we resort to the effective 1D approach, given its success in both tetratomic and mass-imbalanced hexatomic problems.

In the center-of-mass frame, three identical molecules $(\mathbf{r}_1, \mathbf{r}_2, \mathbf{r}_3)$ can be described by two relative coordinates $\mathbf{r} = \mathbf{r}_2 - \mathbf{r}_1$ and $\boldsymbol{\rho} = (2/\sqrt{3})[\mathbf{r}_3 - (\mathbf{r}_1 + \mathbf{r}_2)/2]$, whose deviations from y direction give four fluctuation variables $\{\delta\theta_r, \delta\phi_r, \delta\theta_\rho, \delta\phi_\rho\}$. The expansion of $H^{(3)}(\mathbf{r}, \boldsymbol{\rho})$ up to the lowest fluctuation order leads to two sets of coupled harmonic oscillators in terms of $\{\delta\theta_r, \delta\theta_\rho\}$ and $\{\delta\phi_r, \delta\phi_\rho\}$. Their zero-point energies comprise the repulsive force for three molecules effectively moving along y, denoted as $u^{(3)}$ [47]. Finally, we arrive at the effective 1D model $H^{(3)}_{\rm 1D} = -(\hbar^2/m)[(\partial^2/\partial y_r^2) + (\partial^2/\partial y_\rho^2)] + U^{(3)}(y_r, y_\rho)$, with

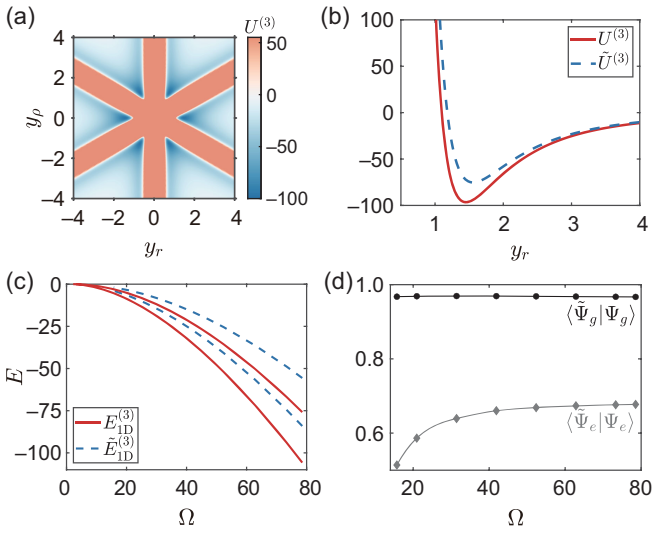

FIG. 5. Effective potential and wave functions of three identical molecules. (a) Effective 1D potential $U^{(3)}$ [Eq. (7)] in (y_r, y_ρ) plane at $\hbar\Omega/E_u = 52$. (b) $U^{(3)}$ and $\tilde{U}^{(3)}$ as functions of y_r at a fixed $y_\rho = 0$ (corresponding to three equally spaced molecules). (c) Energy spectra from $U^{(3)}$ (solid) and $\tilde{U}^{(3)}$ (dashed). (d) Wave function overlap for the ground and excited states of two models. The units of length, energy, and Ω are, respectively, l_u, E_u, and $E_u/\hbar$.

$$U^{(3)} = -4C_3\left(\frac{1}{|y_r|^3} + \frac{1}{|y_-|^3} + \frac{1}{|y_+|^3}\right) + u^{(3)}(y_r, y_\rho), \tag{7}$$

where $y_r = y_2 - y_1$ and $y_\rho = (2/\sqrt{3})[y_3 - (y_1 + y_2)/2]$ are the projections of $\mathbf{r}$ and $\boldsymbol{\rho}$ along y, respectively, and $y_\pm = (y_r/2) \pm [\sqrt{3}y_\rho/2]$. Figure 5(a) shows the typical structure of $U^{(3)}(y_r, y_\rho)$, which fully respects exchange symmetry under $y_i \leftrightarrow y_j$.

We have solved hexatomic bound states by exactly diagonalizing $H^{(3)}_{\rm 1D}$ in discretized (y_r, y_ρ) space. The binding energies of the two lowest hexatomic states as functions of Ω are shown in Fig. 2. Remarkably, these states are generally much deeper than tetratomic ones: for the ground state, its binding energy is even beyond twice the tetratomic case. In addition, all these states obey Bose-Fermi duality, as shown by $\Psi^{(3)}(y_r, y_\rho)$ in Figs. 3(c1) and 3(c2). This, again, is protected by $\sim r^{-4}$ repulsion in $u^{(3)}$, which prohibits two molecules coming close together. The resulting crystalline pattern of three molecules can be detected from $G_2(y)$, as shown in Fig. 3(e).

To gain a physical picture for hexatomic binding, we consider a decomposed form of interaction potential,

$$\tilde{U}^{(3)} = U^{(2)}(y_r) + U^{(2)}(y_-) + U^{(2)}(y_+). \tag{8}$$

$\tilde{U}^{(3)}$ can be a good approximation for $U^{(3)}$ [see Fig. 5(b)], and importantly, it inspires us to construct hexatomic states

from tetratomic ones. To be concrete, for three molecules aligning along y with $y_1 < y_2 < y_3$, the 1D Hamiltonian under $\tilde{U}^{(3)}$ can be written as [47]

$$\tilde{H}^{(3)}_{1D} = H^{(2)}_{1D}(y_{12}) + H^{(2)}_{1D}(y_{23}) + h'(y_{12}, y_{23}), \quad (9)$$

where $y_{ij} \equiv y_j - y_i$, $H^{(2)}_{1D}$ is given in (3), and $h'(y, y') = -(\hbar^2/m)(\partial/\partial y)(\partial/\partial y') + U^{(2)}(y + y')$. In Eq. (9), two $H^{(2)}_{1D}$ give neighboring tetratomic states, while h' builds long-range correlation between them. Take two tetratomic levels $\Psi^{(2)}_g$ and $\Psi^{(2)}_e$, we then expand $\tilde{H}^{(3)}$ in the bases $\{\Psi^{(2)}_g(y_{12})\Psi^{(2)}_g(y_{23}), \Psi^{(2)}_g(y_{12})\Psi^{(2)}_e(y_{23}), \Psi^{(2)}_e(y_{12})\Psi^{(2)}_g(y_{23})\}$. The resulting spectra $\tilde{E}^{(3)}_{1D}$ show qualitative agreements with $E^{(3)}_{1D}$ in Fig. 5(c). The ground state wave function, dominated by $\Psi^{(2)}_g(y_{12})\Psi^{(2)}_g(y_{23})$, also matches very well with the full 1D result in Fig. 5(d). This explains why the lowest hexatomic state coexists with the tetratomic state, with binding energy beyond twice the latter due to negative energy correction from h'. For the first excited state, it involves local excitation of one tetratomic state from $\Psi^{(2)}_g$ to $\Psi^{(2)}_e$ [47], and its overlap with the full 1D result is above 60% for $\hbar\Omega/E_u \gtrsim 20$; see Fig. 5(d).

We emphasize that all above bound states are universal, in that their properties only depend on the long-range dipolar strength (with length scale $\sim l_d$) and the microwave coupling [with length scale $l_\Omega \equiv \sqrt{\hbar/(m\Omega)}$]. That is to say, for different polar molecules with the same l_d and l_Ω, they share the same bound state property. This is distinct from Efimov trimers in atomic systems, whose spectrum requires the knowledge of a (short-range) three-body parameter that depends on specific atoms [28,29,54]. With dipolar interactions, it has been shown that the Efimov physics emerges at length scale $l_d \ll r \ll |a_s|$ (a_s is the s-wave scattering length) [44]. Given polar molecules with very large $l_d \gtrsim 10^4 a_0$ [4–9], Efimov trimers are expected to be very shallow and only appear in a narrow window near shape resonance $a_s \to \infty$ [48,49,55,56]. These make Efimov physics extremely difficult to explore, in practice. On the contrary, our universal clusters have typical size $\sim r_m (\ll l_d)$, as located by the minimum of $U^{(2)}$ [Eq. (4)], and thus are much more realistic to probe. In the regime $l_\Omega \ll l_d$, we have $r_m \approx 4\sqrt{2} l_\Omega$ around hundreds of a_0 for typical $\Omega\sim$ tens of megahertz: for instance, $r_m = 428 a_0$ for NaK molecules at $\Omega = (2\pi)10$ MHz. For these universal clusters (of size $\sim r_m$), the effective 1D approach works well and the Bose-Fermi duality can be guaranteed. They should be distinguished from shallow clusters near resonance, where quantum statistics play a significant role and the clusters carry a 3D instead of 1D character [47].

The above analysis of universal clusters can be directly extended to a large ensemble of molecules. For N identical (bosonic or fermionic) molecules, since any neighboring molecules are closely linked along y as tetratomic bound state, the ground state under 1D description would be $\Psi^{(2)}_g(y_{12})\Psi^{(2)}_g(y_{23})\ldots\Psi^{(2)}_g(y_{N-1,N})$ at given order $y_1 < y_2 \ldots < y_N$. The whole system then behaves as an elongated and crystalline self-bound droplet; see Fig. 1(c). The additional long-range correlation between molecules leads to an attractive energy correction that could further stabilize the system [47]. The density crystallization can be probed via $G_2(y)$ [Eq. (5)] using quantum gas microscopes [57–59]. The ground state droplet can undergo local excitations with $\Psi^{(2)}_g(y_{i,i+1}) \to \Psi^{(2)}_e(y_{i,i+1})$, where i is the index of the tetratomic link. By manipulating the locations of $\{i\}$, one could imagine a rich excitation manifold with various crystalline patterns.

Our Letter has revealed unique few-body physics in polar molecules that are substantially different from those in short-range interacting atomic systems. First, the strong dipolar interaction with a large shielding repulsion is shown to favor the formation of universal bound states, whose properties only depend on two physical lengths (l_d and l_Ω). Second, the interaction anisotropy facilitates the effective 1D description and leads to the fascinating property of Bose-Fermi duality, despite the fact that the physical system is in 3D free space. Finally, the many-body implications of these universal clusters are very different from that in atomic systems. Specifically, clusters in the latter case are often viewed as composite particles in driving collective many-body phases [39–43]. However, here the spatially extended clusters cannot be considered as a composite unit. Instead, when adding more molecules to the cluster, it will become a new bigger bound state and finally evolve to a self-bound droplet [Fig. 1(c)].

We expect our results of universal clusters and elongated droplets are generally applicable to finite $\xi(< \pi/4)$, where the microwave field is elliptic enough to support the 1D scenario. In fact, a smaller ξ can efficiently suppress inelastic two-body loss [60] and make the analytical potential in (1) quantitatively more accurate [16]. With a smaller ξ, a bare r^{-6} shielding core will add to the induced r^{-4} repulsion, leading to shallower bound states. In this case, the effective 1D theory can be further improved by incorporating high-order angular fluctuations [61]. Surely, for very small ξ, the 1D scenario will break down. Indeed, a planar crystalline droplet has been predicted recently for $\xi = 0$ [15]. In this way, the ellipticity (ξ) serves as an efficient parameter to control the effective dimension of polar molecules. In the future, it will be interesting to study ξ-driven dimensional crossover of distinct crystalline states, as well as the effect of dual microwave fields in bosonic molecules [62,63].

Acknowledgments—We thank Mingyuan Sun, Ruijin Liu, Peng Zhang, and Tao Shi for useful discussions and Andreas Schindewolf, Bo Zhao, and Pengjun Wang for

helpful feedback on the manuscript. This work is supported by National Natural Science Foundation of China (92476104, 12525412, 12134015) and Quantum Science and Technology-National Science and Technology Major Project (2024ZD0300600). T. S. is thankful for support from the Postdoctoral Fellowship Program of CPSF (Grant No. GZC20232945).

Data availability—The data that support the findings of this article are openly available [64].

[1] T. Karman and J. M. Hutson, Microwave shielding of ultracold polar molecules, Phys. Rev. Lett. **121**, 163401 (2018).
[2] L. Lassabliere and G. Quemener, Controlling the scattering length of ultracold dipolar molecules, Phys. Rev. Lett. **121**, 163402 (2018).
[3] L. Anderegg, S. Burchesky, Y. Bao, S. S. Yu, T. Karman, E. Chae, K.-K. Ni, W. Ketterle, and J. M. Doyle, Observation of microwave shielding of ultracold molecules, Science **373**, 779 (2021).
[4] A. Schindewolf, R. Bause, X.-Y. Chen, M. Duda, T. Karman, I. Bloch, and X.-Y. Luo, Evaporation of microwave-shielded polar molecules to quantum degeneracy, Nature (London) **607**, 677 (2022).
[5] X.-Y. Chen, A. Schindewolf, S. Eppelt, R. Bause, M. Duda, S. Biswas, T. Karman, T. A. Hilker, I. Bloch, and X.-Y. Luo, Field-linked resonances of polar molecules, Nature (London) **614**, 59 (2023).
[6] X.-Y. Chen, S. Biswas, S. Eppelt, A. Schindewolf, F. Deng, T. Shi, S. Yi, T. A. Hilker, I. Bloch, and X.-Y. Luo, Ultracold field-linked tetratomic molecules, Nature (London) **626**, 283 (2024).
[7] J. Lin, G. Chen, M. Jin, Z. Shi, F. Deng, W. Zhang, G. Quéméner, T. Shi, S. Yi, and D. Wang, Microwave shielding of bosonic NaRb molecules, Phys. Rev. X **13**, 031032 (2023).
[8] N. Bigagli, C. Warner, W. Yuan, S. Zhang, I. Stevenson, T. Karman, and S. Will, Collisionally stable gas of bosonic dipolar ground state molecules, Nat. Phys. **19**, 1579 (2023).
[9] N. Bigagli, W. Yuan, S. Zhang, B. Bulatovic, T. Karman, I. Stevenson, and S. Will, Observation of Bose-Einstein condensation of dipolar molecules, Nature (London) **631**, 289 (2024).
[10] S. Zhang, W. Yuan, N. Bigagli, H. Kwak, T. Karman, I. Stevenson, and S. Will, Observation of self-bound droplets of ultracold dipolar molecules, arXiv:2507.15208.
[11] Z. Shi, Z. Huang, F. Deng, W.-J. Jin, S. Yi, T. Shi, and D. Wang, Bose-Einstein condensate of ultracold sodium-rubidium molecules with tunable dipolar interactions, arXiv:2508.20518.
[12] W. Jin, F. Deng, S. Yi, and T. Shi, Bose-Einstein condensates of microwave-shielded polar molecules, Phys. Rev. Lett. **134**, 233003 (2025).
[13] W. Zhang, K. Chen, S. Yi, and T. Shi, Quantum phases for finite-temperature gases of bosonic polar molecules shielded by dual microwaves, PRX Quantum **6**, 040307 (2025).
[14] T. Langen, J. Boronat, J. Sanchez-Baena, R. Bombin, T. Karman, and F. Mazzanti, Dipolar droplets of strongly interacting molecules, Phys. Rev. Lett. **134**, 053001 (2025).
[15] M. Ciardi, K. R. Pedersen, T. Langen, and T. Pohl, Self-bound monolayer crystals of ultracold polar molecules, Phys. Rev. Lett. **135**, 153401 (2025).
[16] F. Deng, X.-Y. Chen, X.-Y. Luo, W. Zhang, S. Yi, and T. Shi, Effective potential and superfluidity of microwave-shielded polar molecules, Phys. Rev. Lett. **130**, 183001 (2023).
[17] A. V. Avdeenkov and J. L. Bohn, Linking ultracold polar molecules, Phys. Rev. Lett. **90**, 043006 (2003).
[18] A. V. Avdeenkov, D. C. E. Bortolotti, and J. L. Bohn, Field-linked states of ultracold polar molecules, Phys. Rev. A **69**, 012710 (2004).
[19] G. Quéméner, J. L. Bohn, and James F. E. Croft, Electro-association of ultracold dipolar molecules into tetramer field-linked states, Phys. Rev. Lett. **131**, 043402 (2023).
[20] B. Mukherjee, M. D. Frye, C. R. Le-Sueur, M. R. Tarbutt, and J. M. Hutson, Shielding collisions of ultracold CaF molecules with static electric fields, Phys. Rev. Res. **5**, 033097 (2023).
[21] B. Xu, F. Yang, R. Qi, H. Zhai, and P. Zhang, Synthetic mutual gauge field in microwave-shielded polar molecular gases, Phys. Rev. Res. **7**, L032027 (2025).
[22] J. Dutta, B. Mukherjee, and J. M. Hutson, Universality in the microwave shielding of ultracold polar molecules, Phys. Rev. Res. **7**, 023164 (2025).
[23] S.-J. Huang, Y.-T. Hsu, H. Lee, Y.-C. Chen, A. G. Volosniev, N. T. Zinner, and D.-W. Wang, Field-induced long-lived supermolecules, Phys. Rev. A **85**, 055601 (2012).
[24] I. Stevenson, S. Singh, A. Elkamshishy, N. Bigagli, W. Yuan, S. Zhang, C. H. Greene, and S. Will, Three-body recombination of ultracold microwave-shielded polar molecules, Phys. Rev. Lett. **133**, 263402 (2024).
[25] E. Braaten and H.-W. Hammer, Universality in few-body systems with large scattering length, Phys. Rep. **428**, 259 (2006).
[26] C. H. Greene, P. Giannakeas, and J. Pérez-Ríos, Universal few-body physics and cluster formation, Rev. Mod. Phys. **89**, 035006 (2017).
[27] P. Naidon and S. Endo, Efimov physics: A review, Rep. Prog. Phys. **80**, 056001 (2017).
[28] V. N. Efimov, Weakly-bound states of three resonantly interacting particles, Yad. Fiz. **12**, 1080 (1970).
[29] V. N. Efimov, Energy levels of three resonantly interacting particles, Nucl. Phys. **A210**, 157 (1973).
[30] O. I. Kartavtsev and A. V. Malykh, Low-energy three-body dynamics in binary quantum gases, J. Phys. B **40**, 1429 (2007).
[31] D. Blume, Universal four-body states in heavy-light mixtures with a positive scattering length, Phys. Rev. Lett. **109**, 230404 (2012).
[32] B. Bazak and D. S. Petrov, Five-body Efimov effect and universal pentamer in fermionic mixtures, Phys. Rev. Lett. **118**, 083002 (2017).
[33] L. Pricoupenko and P. Pedri, Universal $(1+2)$-body bound states in planar atomic waveguides, Phys. Rev. A **82**, 033625 (2010).

[34] J. Levinsen and M. M. Parish, Bound states in a quasi-two-dimensional Fermi gas, Phys. Rev. Lett. **110**, 055304 (2013).
[35] R. Liu, C. Peng, and X. Cui, Universal tetramer and pentamer in two-dimensional fermionic mixtures, Phys. Rev. Lett. **129**, 073401 (2022).
[36] O. I. Kartavtsev, A. V. Malykh, and S. A. Sofianos, Bound states and scattering lengths of three two- component particles with zero-range interactions under one-dimensional confinement, J. Exp. Theor. Phys. **108**, 365 (2009).
[37] N. P. Mehta, Born-Oppenheimer study of two-component few-particle systems under one-dimensional confinement, Phys. Rev. A **89**, 052706 (2014).
[38] A. Tononi, J. Givois, and D. S. Petrov, Binding of heavy fermions by a single light atom in one dimension, Phys. Rev. A **106**, L011302 (2022).
[39] S. Endo and A. M. García-García, and P. Naidon, Universal clusters as building blocks of stable quantum matter, Phys. Rev. A **93**, 053611 (2016).
[40] R. Liu, W. Wang, and X. Cui, Quartet superfluid in two-dimensional mass-imbalanced Fermi mixtures, Phys. Rev. Lett. **131**, 193401 (2023).
[41] C. J. M. Mathy, M. M. Parish, and D. A. Huse, Trimers, molecules, and polarons in mass-imbalanced atomic Fermi gases, Phys. Rev. Lett. **106**, 166404 (2011).
[42] M. M. Parish and J. Levinsen, Highly polarized Fermi gases in two dimensions, Phys. Rev. A **87**, 033616 (2013).
[43] R. Liu, C. Peng, and X. Cui, Emergence of crystalline few-body correlations in mass-imbalanced Fermi polarons, Cell Rep. Phys. Sci. **3**, 100993 (2022).
[44] Y. Wang, J. P. D'Incao, and C. H. Greene, Efimov effect for three interacting bosonic dipoles, Phys. Rev. Lett. **106**, 233201 (2011).
[45] Y. Wang, J. P. D'Incao, and C. H. Greene, Universal three-body physics for fermionic dipoles, Phys. Rev. Lett. **107**, 233201 (2011).
[46] K. Oi, P. Naidon, and S. Endo, Universality of Efimov states in highly mass-imbalanced cold-atom mixtures with van der Waals and dipole interactions, Phys. Rev. A **110**, 033305 (2024).
[47] See Supplemental Material at http://link.aps.org/supplemental/10.1103/hcwf-tk6c for more details on the derivations of effective 1D models and the properties of tetratomic and hexatomic bound states.
[48] K. Kanjilal and D. Blume, Low-energy resonances and bound states of aligned bosonic and fermionic dipoles, Phys. Rev. A **78**, 040703(R) (2008).
[49] V. Roudnev and M. Cavagnero, Resonance phenomena in ultracold dipole–dipole scattering, J. Phys. B **42**, 044017 (2009).
[50] Y. Wang and C. H. Greene, Universal bound and scattering properties for two dipoles, Phys. Rev. A **85**, 022704 (2012).
[51] M. D. Girardeau, Relationship between systems of impenetrable bosons and fermions in one dimension, J. Math. Phys. (N.Y.) **1**, 516 (1960).
[52] T. Cheon and T. Shigehara, Fermion-boson duality of one-dimensional quantum particles with generalized contact interactions, Phys. Rev. Lett. **82**, 2536 (1999).
[53] A. C. Fonseca, E. F. Redish, and P. E. Shanley, Efimov effect in an analytically solvable model, Nucl. Phys. **A320**, 273 (1979).
[54] M. Berninger, A. Zenesini, B. Huang, W. Harm, H.-C. Nägerl, F. Ferlaino, R. Grimm, P. S. Julienne, and J. M. Hutson, Universality of the three-body parameter for Efimov states in ultracold cesium, Phys. Rev. Lett. **107**, 120401 (2011).
[55] M. Marinescu and L. You, Controlling atom-atom interaction at ultralow temperatures by dc electric fields, Phys. Rev. Lett. **81**, 4596 (1998).
[56] Z.-Y. Shi, R. Qi, and H. Zhai, *s*-wave scattering resonances induced by dipolar interactions of polar molecules, Phys. Rev. A **85**, 020702(R) (2012).
[57] T. de-Jongh, J. Verstraten, M. Dixmerias, C. Daix, B. Peaudecerf, and T. Yefsah, Quantum gas microscopy of fermions in the continuum, Phys. Rev. Lett. **134**, 183403 (2024).
[58] J. Xiang, E. Cruz-Colón, C. C. Chua, W. R. Milner, J. deHond, J. F. Fricke, and W. Ketterle, In situ imaging of the thermal de Broglie wavelength in an ultracold Bose gas, Phys. Rev. Lett. **134**, 183401 (2025).
[59] R. Yao, S. Chi, M. Wang, R. J. Fletcher, and M. Zwierlein, Measuring pair correlations in Bose and Fermi gases via atom-resolved microscopy, Phys. Rev. Lett. **134**, 183402 (2025).
[60] T. Karman and J. M. Hutson, Microwave shielding of ultracold polar molecules with imperfectly circular polarization, Phys. Rev. A **100**, 052704 (2019).
[61] H. Wang, T. Shi, and X. Cui, Interaction-induced dimension reduction for bound states in microwave-shielded ultracold molecules, arXiv:2511.09856.
[62] F. Deng, X. Hu, W. Jin, S. Yi, and T. Shi, Two- and many-body physics of ultracold molecules dressed by dual microwave fields, Nat. Commun. **16**, 11219 (2025).
[63] T. Karman, N. Bigagli, W. Yuan, S. Zhang, I. Stevenson, and S. Will, Double microwave shielding, PRX Quantum **6**, 020358 (2025).
[64] T. Shi, H. Wang, and X. Cui, Data for Universal bound states with Bose-Fermi duality in microwave-shielded ultracold molecules, 2025, 10.6084/m9.figshare.29306735.v4.